小野の稿を参照されたい．

当研究所，変異遺伝部と総合評価研究室は，我が国の既存化学物質データベースからエームス試験データを有する206化学物質についてDEREK，MultiCASE，ADMEWORKSを用いてその予測性を評価した[7]（Table 1）．予測の評価は感度（Sensitivity；エームス陽性物質を陽性と判定する能力），特異性（Specificity；エームス陰性物質を陰性と判定する能力），および一致性（Concordance；陽性および陰性の一致率）を指標として行った．表が示すように感度が最も高かったものがDEREKとADMEWORKS（73.1%），特異性が最も高かったものがMultiCASE（91.1%），一致率ではDEREK（86.4%）が最も高かった．ADMEWORKSは特異性が69.7%と低く，このことは多くのエームス陰性物質の約3割を間違って陽性と判定する（False positive）ことを意味する．同様の傾向は，英国のKirklandが報告した703のエームス試験を含む*in vitro*遺伝毒性試験データベース（CGX database）での評価結果からも得られた[7,8]．一方，Snyderらは2002年～2004年のPhysicians' Desk Referenceに収載の医薬品からエームス試験データがある394品目を抽出し，DEREK，MultiCASE，TOPKAT（ADMEWORKSと同様の人工知能型QSARモデル）の3種類のSARモデルを用いて試験結果の予測を行ったところ，MultiCASE，TOPKATは比較的高い特異性を示したが，感度は50%以下であった[9]．また，DEREKにおいては感度，特異性とも低く一致率は3つの中で最低であった．医薬品と工業化学物質では化学構造に含まれるSAに特徴があるため異なった結果になったものと予測される．いずれにせよここでのSAR利用の目的は遺伝毒性可能性物質のスクリーニングであり，できるだけ感度を上げ，偽陰性（False negative）を減らすモデルの構築，改良が重要である．

SARモデルの組合せによる予測率の向上と，化学物質の優先付けへの適用

DEREK，MultiCASE，ADMEWORKSの3つのSARモデルはそれぞれ異なる経験的，数学的，統計的アプローチが取り入れられており，そのエームス試験予測結果も時として異なることは先に述べた．Hayashiらは3つのSARモデルを組み合わせることにより，お互いの欠点を相補し，エームス試験の予測率の向上を図ることに成功した[7]．また，彼らはこれまでの化学物質の安全性評価の経験から，分子量が3,000以上の高分子化合物の大部分はバクテリアの細胞壁を通過することができず，一般にエームス試験陰性であること，例外としてエポキシ基を持つ高分子ポリマーにはエームス陽性を示す化合物が存在することなどを，SARアプローチの前に考慮した決定樹を提唱した（Fig. 2）．これは実際の毒性試験を必要とする化学物質の優先付けや，絞り込みに有用である．3つのSARモデルにおいて2つ以上で陽性もしくは陰性の場合，3つ全てにおいて陽性もしくは陰性の

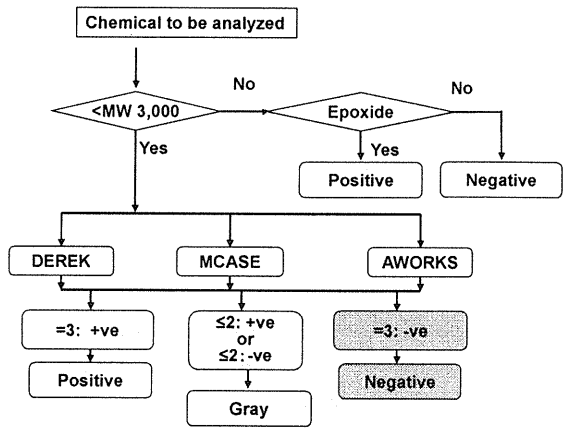

Fig. 2 Decision tree for prioritizing chemicals for consequent experimental verification. MCASE: MultiCASE, AWORKS: ADMEWORKS

Table 1 Performance of SAR models for the Ames test (Hayashi et al., 2005)

	Ames Results	+	-	Total	Sensitivity (%)	Specificity (%)	Concordance (%)
DEREK	+	19	7	26			
	-	21	159	180			
	Total	40	166	206	73.1	88.3	86.4
MCASE	+	13	20	20			
	-	13	146	146			
	Total	26	166	166	65.0	91.1	88.0
AWORKS	+	19	26	26			
	-	54	178	178			
	Total	73	204	204	73.1	69.7	70.1

MCASE: MultiCASE; AWORKS: ADMEWORKS

場合にカテゴリー化することにより予測率を向上させることができる．後者の場合，感度87%，特異性95%，一致率94%と予測率は格段に向上した（Table 2）．一方，すべての化学物質は予測結果の違いからこのようなカテゴリーの中に入るわけではない．当然適応される化学物質の割合（Applicability）は低下し，先の場合は約半分程度（55%）となる．しかしながら，現在，年間10トン以上生産されている既存化学物質は我が国で20,000種類以上も存在し，そのうち約90%である18,000種類の化学物質についてはエームス試験さえ実施されていない状況を考えると，9,900種類（18,000×0.55）の化学物質の絞り込みには依然として重要ある．

他の *in vitro* 遺伝毒性の予測

染色体異常試験はエームス試験と同様に化学物質の承認及び登録における安全性確認に重要な*in vitro*遺伝毒性試験項目の一つである．染色体異常試験についてもSARモデルが開発されているが，染色体異常は化学物質とDNAの直接的相互作用に加え，DNA複製に関する酵素（トポイソメラーゼ等）や，染色体分配に関与する核タンパク質（ヒストンタンパク質等）との相互作用などのメカニズムによっても誘発されるため，より複雑である．また，染色体異常自体も，分裂中期における染色体の構造的特性の結果として観察可能となるため，上記の全てのメカニズムが染色体異常として認識されるわけではない．従って，染色体異常を引き起こす化学物質の予測のためのモデル化には多様な計算的アプローチが必要である．また，エームス試験と比較して，SAの抽出に必要な実験データベースは少ない．

知識ベースのSARモデルであるDEREK（バージョン11）には74種類の染色体異常試験陽性のSAが収納されている（エームス試験は87種類）．エームス試験と同様に209の既存化学物質に関する染色体異常試験の予測性を評価した（Table 3）．感度，特異性，一致性とも全てエームス試験に劣り，特に感度は64%であった．このことは36%の染色体異常誘発物質を予測できないことを示す（False negative）．染色体異常試験結果自体が，げっ歯類発がん性試験結果と相関性が低いことも指摘されており，一部の染色体異常陽性結果は遺伝毒性発がん性と無関係であるのかもしれない．染色体異常試験の予測性の向上にはSARモデルの改良と，染色体異常試験自体の改良の両者が必要である．

化学物質は薬物代謝によって活性化され遺伝毒性を発現するものが少なくない．*In vitro*遺伝毒性試験の場合，通常ラット肝臓から調製されたミクロゾーム分画（S9）を試験化合物と同時に加えることにより，予測される肝臓での代謝物の評価を同時に行っている．親化合物の化学構造と遺伝毒性作用との関連性が低い場合，薬物代謝による活性化体の関与が考えられる．代謝に起因する毒性発現の複雑さはSAR研究では厄介である．ブルガス大学のMekenyanらは，ラット肝S9での代謝反応，および非生物的反応の総合的ライブラリーと，代謝による変換確率の推定値を用いて妥当な代謝マップを創り出す帰納的アルゴリズムを開発した[10]．これは組織代謝シミュレータ（TIssue MEtabolite Simulator；TIMES）と呼ばれている．既存の文献データから得られた薬物代謝に関する変換率の情報を用いて，特定の基準条件に対して変換確率を較正することができ，また，データがない場合は組み合わせアルゴリズムを用い，既知の代謝マップを適合性が最も高い変換確率に書き換えることができ

Table 2 Performance of combined SAR model for the Ames test (Hayashi et al., 2005)

Combination of 3 SARs		+++	---	Total	Sensitivity (%)	Specificity (%)	Concordance (%)
Ames	+	13	2	15			
	-	5	94	99			
	Total	18	96	114*	86.7	94.9	55.3

*Among 206 chemicals, 114 chemicals were categorized into +++ or ---.
Applicability 55.3% (114/206).

Table 3 Performance of DEREK for the chromosome aberration test

DEREK		+	-	Total	Sensitivity (%)	Specificity (%)	Concordance (%)
Chrom	+	60	34	94			
Ab	-	29	86	115			
	Total	89	120	209	63.8	74.8	69.9

Chorm Ab: Chromosome aberration test

る．実際のTIMESソフトウェアでは代謝物の予測だけでなく，彼らによって同じく開発されたQSARモデルであるOASIS（Optimized Approach Based on Structural Indices Set）との組合せによって，個々の代謝物のエームス試験，染色体異常試験結果まで予測することができる．

おわりに

(Q)SARモデルの*in vitro*遺伝毒性試験の予測に関して本稿で述べた．しかしながら，*in vitro*遺伝毒性試験自体が発がん性化学物質の予測を目的とするスクリーニング試験であることを考えると，スクリーニング試験の結果の予測を行うことにどれだけの科学的な価値があるか，疑問に思われるかも知れない．医薬品を始め，多くの化学物質の安全性評価のためにエームス試験，染色体異常試験が法律で義務づけられており，多数の候補化合物や，既存化学物質の中から優先度の高い物質を選択するツールとして(Q)SARは現実的に極めて有効である．しかしながら，(Q)SAR研究の本質はツールとしての利用ではない．始めに述べたように（Q)SARはMillerの唱えた発がん化学物質の求電子理論により，エームス試験というバイオアッセイの結果を証明することから始まった．この思想は分子レベルで生命現象，特に毒性メカニズム解明を試みた最初の例である．ほとんど全ての毒性はエームス試験のように単純では無く，極めて複雑であり，またメカニズムが不明である．2007年から米国EPAが中心となって開始したToxCastプログラムでは*in vitro*試験系から多くの毒性経路やメカニズムを抽出し，(Q)SARに組み入れる手法を開発する[11]．成功すれば，Millerのように様々の毒性を分子レベルで解明できるかも知れない．それが（Q)SARとコンピュータトキシコロジーの最終目標であり，その利用が科学的知見に基づく化学物質の真のリスク評価に通じるものであると信じる．我が国でも同様のプロジェクトを立ち上げ，毒性学の未来を切り開く努力が必要である．

参考文献

1）Schmit, O.: *Physik Chem B42*, 83 (1939)
2）Pullman, A. and Pullman, B.: *Rev Sci 3*, 117 (1946)
3）Miller, J.A. and Miller, E.C.: *Cancer 47*, 2327-2345 (1981)
4）Ames, B.N., *Cancer 53*, 2030-2040 (1984)
5）Ashby, J. and Tennant, R.W.: *Mutat Res 204*, 17-115 (1988)
6）Benigni, R. and Bossa , C: *Mutat Res, 659*, 248-261 (2008)
7）Hayashi, M., Kamata, E., Hirose, A., Takahashi, M., Morita, T., and Ema, M.: *Mutat Res, 588*, 129-135 (2005)
8）Kirkland, D., Aardema, M., Henderson, L., and Muller, L.: *Mutat Res, 584*, 1-256 (2005)
9）Snyder, R., Pearl, G., Mandakas, Choy, W., Goodsaid, F., and Rosenblum, I.: *Environ Mol Mutgen 43*, 143-158 (2004)
10）Mekenyan, O.G., Dimitrov, S.D., Pavlov, T.S., and Veith, G.D.: *Curr Pharm Des 10*, 1273-1293 (2004)
11）Schmit, C.W.: *Environ Health Perspect, 117*, A349-A352 (2009)

Bull. Natl. Inst. Health Sci., **128**, 44-49 (2010) **Special Report**

4）*in vivo*反復投与毒性の構造活性相関による予測評価の展望

小野 敦

Perspective of predictive toxicity assessment of *in vivo* repeated dose toxicity using structural activity relationship

Atsushi Ono

Tens of thousands of existing chemicals have been widely used for manufacture, agriculture, household and other purposes in worldwide. Only approximately 10% of chemicals have been assessed for human health hazard. The health hazard assessment of residual large number of chemicals for which little or no information of their toxicity is available is urgently needed for public health. However, the conduct of traditional toxicity tests which involves using animals for all of these chemicals would be economically impractical and ethically unacceptable. (Quantitative) Structure-Activity Relationships [(Q)SARs] are expected as method to have the potential to estimate hazards of chemicals from their structure, while reducing time, cost and animal testing currently needed. Therefore, our studies have been focused on evaluation of available (Q)SAR systems for estimating *in vivo* repeated toxicity on the liver. The results from our preliminary analysis showed the distribution for LogP of the chemicals which have potential to induce liver toxicity was bell-shape and indicating the possibility to estimate liver toxicity of chemicals from their physicochemical property. We have developed (Q)SAR models to *in vivo* liver toxicity using three commercially available systems (DEREK, ADMEWorks and MultiCASE) as well as combinatorial use of publically available chemoinformatic tools (CDK, MOSS and WEKA). Distinct data-sets of the 28-day repeated dose toxicity test of new and existing chemicals evaluated in Japan were used for model development and performance test. The results that concordances of commercial systems and public tools were almost same which below 70% may suggest currently attainable knowledge of *in silico* estimation of complex biological process, though it possible to obtain complementary and enhanced performance by combining predictions from different programs. In future, the combinatorial application of *in silico* and *in vitro* tests might provide more accurate information which support regulatory decisions. At the same time, an appropriate strategy to use (Q)SAR for of the efficiency and accuracy in chemical management is necessary.

Keywords; Quantitative Structure-Activity Relationships, repeated dose toxicity, liver, existing chemicals, risk assessment

1．はじめに

現在，日本国内では約10万種もの化学物質が様々な用途で流通していると言われている．そのうち，医薬品や農薬など用途ごとに規制されている物質以外の一般化学物質については，主に「化学物質の審査及び製造等の規制に関する法律」（以下「化審法」）により規制される．化審法では，新規の化学物質が製造・輸入される際には，物性（分解性・蓄積性），人への毒性及び生態毒性について，それぞれ定められた試験による審査が行われており，人への毒性に関しては「細菌を用いる復帰突然変異試験」，「ほ乳類培養細胞を用いる染色体異常試験またはマウスリンフォーマTK試験」及び「28日間反復毒性試験」の３種のスクリーニング毒性試験による安全性

To whom correspondence should be addressed:
Atsushi Ono: 1-18-1 Kamiyoga, Setagaya-ku, Tokyo 158-8501, Japan; Tel: +81-3-3700-1429; Fax: +81-3-3700-1408; E-mail: atsushi@nihs.go.jp

評価が実施されている．一方，昭和48年の化審法制定以前から流通していた化学物質（既存化学物質）については，国で必要な試験を実施して安全性評価を進めているが，我が国だけでも数万種の既存化学物質が流通しており，これまでに安全性評価が終了した化学物質はごく一部に過ぎず，残された既存化学物質は人への安全性について不明のまま流通している．それらの化学物質が直ちに問題を起こすことはないとしても潜在的なリスクとなっており，国民の健康を守るためには早急な安全性の評価が望まれるが，数万種の化学物質について従来実施されている毒性試験を実施するのは必要となる費用や期間の面から現実的ではなく，特に動物試験については動物愛護の観点からもなるべく最小限に留める事が求められており，効率的で信頼性の高い新たな安全性評価手法の確立が望まれている．近年，既に毒性試験が実施されている構造類似物質の毒性情報から評価物質の毒性を類推するカテゴリーアプローチ，さらには，化学物質構造と毒性発現との相関から化学物質の毒性を予測する（定量的）構造活性相関（(Quantitive) Stracture Activity Relationship）手法が解決策の一つとして期待されており，世界各国で検討が進められている[1]．化学物質の構造から毒性を予測することが出来れば，毒性試験未実施の化学物質についても安全管理が可能となり，毒性試験を必要とする化学物質の優先順位付けや絞り込みを行うことで効率的な安全性評価が可能となる．さらに将来的には，予測精度の向上により試験そのものが必要なくなる日も来るかもしれない．

2．構造が類似する化学物質からの毒性予測

(Q)SARの基礎は「類似の構造をもつ化学物質は類似の生理活性を生じる」という概念である．医薬品開発のエキスパートは，化学構造から"既知の"薬効や物性をある程度推測出来るという話もあるが，毒性に関してはどうであろうか？　Fig. 1に示す9種のクロロニトロベンゼンの同族体は，いずれも既存化学物質である．これらのうち物質4（2,4-ジクロロニトロベンゼン（CAS No. 611-06-3））については，既存点検による「ラットを用いた反復経口投与毒性・生殖発生毒性併合試験」が実施されており，その結果，血液，腎臓，肝臓への障害が認められ，NOEL 8mg/kg/day未満と報告されている．また，物質2（1,4-ジクロロ-2-ニトロベンゼン（CAS No. 89-61-2））については，既存点検による「ラットを用いる経口投与簡易生殖毒性試験」結果から雌の生殖に関するNOEL 20 mg/kg/dayと報告がある．物質1と3については，毒性試験は実施されてはいないが，物質1～4は化審法では区別されておらず，ジクロロニトロベンゼンとしていずれも第2種監視物質に指定されている．一方，物質9（ペンタクロロニトロベンゼン（CAS No. 82-68-8））は，過去に土壌殺菌剤，防かび剤，防汚剤に使用されていた農薬で，ビーグル犬を用いた混餌投与による2年間慢性毒性試験により胆汁うっ滞性肝障害などからNOEL 0.75 mg/kg/dayと報告されている．この物質は，農薬としては販売禁止となっており厳しい残留基準が定められている．では，物質5～8はどうであろう．これらの物質について毒性試験は実施されていない．しかし，物質構造から物質1～4及び9と同程度の毒性が懸念されないだろうか．もちろん，予想外に毒性が低い可能性も否定出来ない．ここで問題なのは，これらの物質のように安全性未評価の既存化学物質は毒性試験が実施されない限り，特に規制も受けずに流通可能なことである．環境中に一度大量に排出されてしまった化学物質を除去するのは非常に困難であるが，安全性未評価の化合物について一律に厳しい規制を実施するのは現実的ではない．カテゴリーアプローチや(Q)SAR手法による安全性評価スキームが実用化されれば，毒性試験が実施されていない化学物質についても適切な管理を行うことが可能である．Fig. 1の物質群については，化学物質の毒性評価についてある程度の経験があれば，その毒性を疑うであろう．しかし，経験に基づく評価は，評価者によって判断が違ってしまう可能性があるため安全性評価に用いるためには，評価基準が明示的に示されている必要がある．化学構造と毒性との関係については，1970年代から研究されている．1972年にCramerらは，82化合物の構造とNOELデータの解析結果から化学物質の毒性を3クラスに分類する33の構造ルールからなるYes/No型の決定樹を発表している[2]．さらに，1996年Munroらは600以上の化学物質のNOELによるCramer

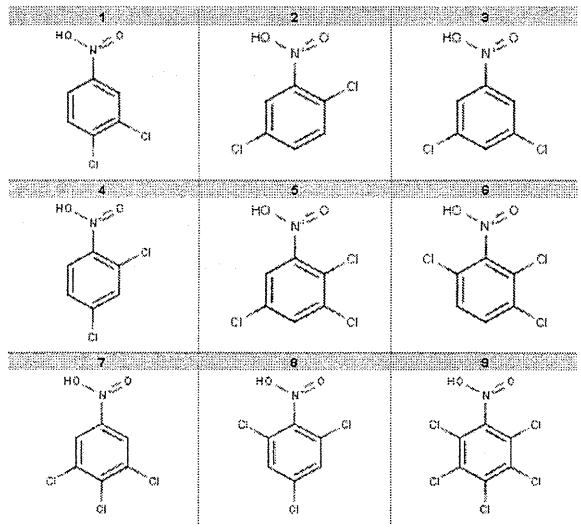

Fig. 1　Structurally similar nine chloronitrobenzene homologs

ruleの検証を行い新たに５つのルールを追加した[3]．JECFAでは毒性情報が無い既存食品香料の安全性評価におけるMunroらの修正Cramer ruleの適用を検討している[4]．Cramer ruleでは，Fig. 1の物質は全てクラス３（強い毒性が懸念される物質）と判定される．

３．化学物質の物理化学的性質と毒性

(Q)SARでは，化学物質の構造そのものだけでなく化学構造から計算可能な様々な物理化学的性質や化学構造の情報を数値化して記述子として予測に用いる．化学物質が生理活性を生じるためには，生体に吸収され，作用部位に到達する必要がある．化学物質の腸管吸収性や細胞膜透過性は，医薬品開発においてバイオアベイラビリティーの向上に重要であり，数多くの研究から化学物質の脂溶性すなわち水／オクタノール分配係数（LogP）との関係が示されている[5,6]．逆に一般化学物質では，吸収率が高ければ経口投与による毒性が発現する可能性が高い．Fig. 2に化審法で実施された28日間反復投与動物試験により肝毒性が認められた物質のLogPの区間分布を示す．上側パネルは，新規化学物質として申請された物質，下側パネルは既存化学物質点検により試験が実施された物質であり，いずれの物質群においても明らかにLogP= ３付近を中心に肝毒性を有する物質の割合が多いことがわかる．しかも，その分布は２つのデータセットでほぼ共通していることから化学物質構造によらない共通ルールであり，化学物質の物理化学的性質からの毒性予測の可能性を示唆している．本来，LogPは実験的に求められる物性値であるが，化学物質の生体内での様々な挙動と関連することから様々な予測計算法が報告されており，今日では，かなりの精度で予測計算が可能である．すなわち，LogP計算こそが構造活性相関の最大の成功例ともいえる．今日では，LogPは多くの構造活性相関モデルでパラメータとして用いられており，経済産業省で検討されている蓄積性予測モデル[7]や環境省で検討されている生態影響予測モデル[8]は，いずれも化学物質を幾つかの構造群に分類し，構造群ごとにLogPとの回帰式をもとに予測を行うものである．しかし，計算により求められるLogPはあくまで予測値であり，化学構造によってアルゴリズム間で異なる値となることに注意が必要である[9]．なお，図２の解析にはLogP予測計算値としてXLogPを用いている[10]．

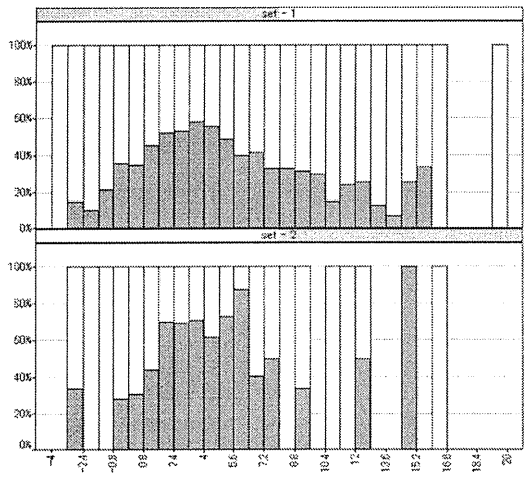

Fig. 2　LogP distribution of liver toxic chemicals X axis showing calculated LogP values (XLogP) and Y axis showing relative percentage of chemicals with (gray) and without (white) the liver toxicity in 28-day repeated dose toxicity test using Rat.: Upper panel (Set-1): Data of newly registered 1227 chemicals for Japanese Chemical Substances Control Law, Lower panel (Set-2): Data of Japanese existing 251 chemicals tested by Ministry of Health, Labour and Welfare.

４．代表的な構造活性相関手法による*in vivo*毒性予測精度の検証

上述の例は，*in vivo*反復毒性についても化学構造や構造から計算可能な性質から予測出来る可能性を示しているが，これまでのところ多岐に渡る化学物質に適用可能な*in vivo*反復毒性について精度の良い（Q)SARモデルは報告されていない．我々の研究室では，これまで化審法における新規化学物質審査や既存化学物質点検における安全性評価を実施するとともに試験データのデータベース化を進めてきており，蓄積されたデータ（化審法データ）をもとに，平成15年度より人健康影響に関する３種のスクリーニング毒性試験についての（Q)SAR評価法の開発を変異遺伝部等との共同により進めており，これまでにAmes試験については国際的評価が高い３種のアプローチの異なるソフトウェアを組み合わせることで実用可能なレベルの予測が可能であることが示された[11]．現在，引き続き染色体異常試験及び28日反復投与毒性試験について検討を進めており，以下にAmes試験予測に用いた３種のソフトウェアを用いて28日反復投与毒性予測の検討を行った結果をそれぞれの手法の特徴とともに示す．

４．１　DEREKによる肝毒性アラートの構築

毒性予測の分野における（Q)SARは，Cramer ruleのように専門家による知見をもとに判断を行うエキスパートシステムと化合構造もしくはその部分構造から計算される物性値などの特徴量を記述子として統計的・情報数理的に解析する手法に分類される．DEREKは，文献情報や有識者により経験的に得られている毒性部位の部分構造（アラート）と経験則をルール化した知識ベースにより，定性的な毒性予測を行うエキスパートシステムである[12]．エキスパートシステムでは，高度な定量予測を

行うのは難しいが，予測の根拠（知識ベース）が容易に確認出来ることやモデル全体の構造を変えることなく知識ベースの追加拡張を行うことが出来る等の利点がある．DEREKを開発したLhasa社は，様々な機関や企業等との共同研究により構築された有害性アラート（部分構造）を知識ベース化してDEREKのアラートとして提供しており，我々はLhasa社と共同で化審法データを基に新規肝毒性アラートの構築を行っている．これまでの研究では，約800化合物の構造情報と毒性試験成績をもとに，(i)化合物構造クラスタリング，(ii)視覚的解析，(iii)関連する毒性に対してのDEREKの既存アラートとの比較により，新たに34個の新規肝毒性Rapid Prototypeアラートの構築に成功している．共同研究を始めた当初，DEREKには40種の肝毒性アラートが搭載されていたが，新規アラートの追加により，アラート構築に用いた学習セット（化審法データ）に対する予測精度は，感度（陽性物質のうち陽性判定された割合）が23％から61％に上昇し，全体の一致率（的中率）も61％から80％に上昇した．しかし，独立した外部データセットによる検証の結果は，感度31％，一致率58％であった．DEREKやCramer ruleのようなエキスパートシステムでは，有害性アラートとの部分構造マッチングにより判定を行うため，有害性アラートがカバーしていない毒性物質は偽陰性判定されてしまう．また，新たに抽出した肝毒性Rapid Prototypeアラートについて解析したところ，幾つかのアラートは非常に少ない物質に由来しており，それらの一部が検証データにおいて非常に多くの物質で偽陽性判定をしていることが一致率の低さの一因であると判断された．現在，構造アラートとのマッチングと分子量やLogPを組み合わせた予測精度向上の検討を進めている．

4．2　ADMEWorksによる肝毒性判別モデルの構築

ADMEWorksは，２次元的分子構造及びクラス特異的部分構造から計算された記述子を使って構築された判別式をもとに毒性評価を行うシステムで，構築済みモジュールにより予測を行うAdmeworksと予測モデル構築を行うモデルビルダーから構成される．モデルビルダーには400種類以上の化合物パラメータ計算モジュールが組み込まれており，部分構造パラメータを含めると数千種のパラメータを発生させることが可能である．P.C.Jursらのグループが開発したADAPT（Automated Data Analysis and Pattern recognition Toolkit）によりSupport Vector Machine（SVM）やAdaBoost（ADA）等の線形判別関数及び線形重回帰モデルを用いた予測を行う[13]．化審法で実施された28日間試験報告書等からモデル構築用にデータ整理が終了した794物質から構造の重複や不正な168物質を除外した626物質をランダムに学習セット：検証セット＝８：２に分割し，モデルビルダーを用いて肝毒性予測モデルを構築し検証を行った．それぞれについて量子力学的パラメータを含む401化学的パラメータと124部分構造パラメータ及び，1000以上の数値変換関数パラメータを利用して，計1631パラメータを発生させ，ADA等によりモデル作成に最適なパラメータの組み合わせを検証して，肝毒性予測に有効な40パラメータを選定した後，SVM，KNN（K Nearest Neighbor）及びADAの３つの判別手法によりモデル構築を行った．学習セット及び検証セットについてのそれぞれの予測手法による予測成績をTable. 1に示した．学習セットではいずれの手法でも80％以上の予測精度が得られたが，検証セットに対する予測では，ADAモデルが一致率70.3％で最も精度が高く，SVM，KNNモデルは，ADAモデルに比べて感度が低い結果であった．

4．3　MultiCASEによる肝毒性予測モデルの構築

Multiple Computer Automated Structure Evaluation（MultiCASE）は，Klopmanらよって開発された独自のCASE理論に基づくシステム[14]であり，入力分子を２～10原子（水素原子を含まない）のフラグメントに分解し，統計処理により有意に活性と相関している部分構造（BIOPHORE）を検出し，同じBIOPHOREを持つ化合物セット内における活性の違いを記述子（MODULATOR）により数値化して活性予測を行う．新規化学物質1231個のデータを学習セットとして28日間試験におけ

Table 1　Comparison of different discriminative methods on the predictive performance of liver toxicity SAR models using ADMEworks

	Training set			Test set		
No. of chemicals*	244/254			53/75		
Discriminator type	SVM	KNN	ADA	SVM	KNN	ADA
Concordance	99.2	83.9	82.9	66.4	62.5	70.3
Sensitivity	100.0	85.7	80.7	24.5	34.0	69.8
Specificity	98.4	82.3	85.0	96.0	82.7	70.7

*Positive for liver toxicity/Negative for liver toxicity

る肝毒性LOAEL値をターゲットとしてモデル構築を行い，既存化学物質251個のデータを検証セットとして予測を行った結果，感度8.7%，特異度89.2%と，ほとんどの化合物が陰性判定される結果となった．MultiCASEでは，ある程度のトレーニングデータが与えられた場合，偽陽性は少ないと考えられるが，学習セット中に評価化合物中のactiveなBIOPHOREが含まれていない場合には，偽陰性となりやすい．そこで，新規化学物質1231個のみを分子量等を基準として学習セット，検証セットに分割し，さらに陰性陽性の判定基準数パターンについてモデル構築を試みた．しかし，あまり一致率の高い結果を得ることは出来ず，一致率は最大で62%，感度は70%に達しなかった．ADMEWorks やMultiCASEのように数学・統計学的手法を用いる手法では定量的なモデル構築が可能で，かつ人為的なバイアスは排除されるが，毒性専門家の経験的な知見を反映することは難しい．また，膨大な数の記述子を機械的に生成して選別を行うため学習の過程で偶然の相関によるモデルが構築される可能性がある．

5．オープンアクセスな構造活性相関ツールの必要性

上記検討に用いたソフトウェアは，いずれも市販のものである．市販ソフトウェアは，優れた機能を有しているが，その一方でモデル構築に用いたソフトウェアを用いずに同じモデルや予測結果を得ることはほとんど不可能であり，さらに継続的な利用のためには，毎年高額なライセンス料が必要となる．今日ではコンピュータの進歩とケモインフォマティックス研究の進展により，様々な化学計算ソフトウェアがオープンソースで開発もしくは無料公開されており，それらを組み合わせて（Q)SARモデルを構築することも可能である．そこで，パブリックで利用可能なツール用いて行った検討結果を以下に示す．MultiCASEで用いたデータセットについて，構造記述子による予測モデルと部分構造による予測モデルの２種類のモデルを構築して予測精度の検討を行った．構造記述子モデルの構築には，The Chemistry Development Kit（CDK）[15] により基本的な構造記述子20個及びXlogP値を計算し，新規物質データを学習セットとしてWeka[16] を用いてRandomForest[17] による予測モデル構築を行い，既存物質データによる検証を行った．RandomForestは，決定木と同じ分類機の一種で，集団学習法と呼ばれ複数の決定木を作成し，これら組み合わせることで精度と汎化力を両立するモデル構築手法である．構造記述子やLogP値は，同一スケールの値ではないため，そのままの値を判別分析や重回帰分析に適用することは出来ない．一方，決定木であればデータへの制約はないが，あまり高精度の分類は期待出来ないため，今回の検討ではRandomForestを用いた．部分構造モデルでは，Molecular Substructure Miner（MOSS）[18] を用いて新規物質1231個を解析して肝毒性物質群に特徴的な部分構造フラグメント111個を抽出した．毒性予測はフラグメントに対する部分構造マッチングではなくフラグメントとの類似性距離（Tanimoto係数）をパラメータとしてRandomForestによる予測モデルを構築して既存物質データによる検証を行った．Table. 2にそれぞれのモデルの学習セット，検証セットでの予測成績を示す．学習セットに対する予測では，いずれのアプローチによってもほぼ100%の一致率を示すモデルが得られたが，検証セットに対する予測一致率はいずれも70%以下であった．得られたモデルの予測精度は良いとは言えないが，前項に示した市販ソフトにより構築したモデルと比べ遜色ない．(Q)SARを広く受け入れられる安全性評価手法として活用していくためには，なるべく多くの人々が安価に利用可能であることが望ましい．我々の研究は，必ずしも独自ツールの開発を目的としてはいないが，パブリックに入手可能なツールを用いて実用可能なモデル構築が可能であるなら，誰でも再現が可能である．もちろん，高精度の予測を行うために特定の市販ソフトウェアが必要不可欠であれば用いるべきである．いずれにせよ，当面の課題は，現時点で実現可能な予測レベルを認識した上で，信頼性向上に向けた検討を進めるとともに，まずは限定的であっても社会的に受用可能な利用法を提案していく中で徐々に適用範囲を広げていくことである．OECDでは，(Q)SARの行政的利用と受け入れの促進に向けた活動を進めており，行政目的で利用される(Q)SARモデルについてアルゴリズムや学習データの公

Table 2 Predictive performance of two different type SAR models for liver toxicity using publically available tools

	Training set		Test set	
No. of chemicals*	515/745		137/117	
Modeltype	Discriptor	Structure	Discriptor	Structure
Concordance	99.9	98.9	66.1	63.4
Sensitivity	99.8	98.1	67.2	62.0
Specificity	100.0	99.5	65.0	65.0

*Positive for liver toxicity/Negative for liver toxicity

開等5項目からなるOECD原則[19]を定めるとともに，加盟各国の提供により各国で蓄積されてきた毒性試験情報や（Q)SARモデル等を統合したOECD QSAR Toolboxの開発を進めている[20]．現在のバージョンのOECD QSAR Toolboxには，人に対する毒性評価モデルとして前述のCramer ruleが登録されている．

6．課題と将来展望

これまでの検討では，いずれの手法により構築した予測モデルにおいても*in vivo*肝毒性について精度の高い予測結果は得られていない．この原因として，学習セットと検証セットに含まれる化学構造の偏りや手法によって適応出来ない化学構造が含まれている可能性が挙げられる．適応化合物の制限や適応性の異なる複数のモデルを組み合わせて利用することでより高精度の予測結果が得られる可能性[11,21]はあるが，別の原因として生体側の反応に関する情報の不足が挙げられる．毒性が化学物質と生体との複雑な相互作用により発現する現象であるのに対して，構造活性相関では化学物質側の特性からの評価しか出来ない．つまり，生体側の情報が不足しているのである．受容体作用のようなターゲット（メカニズム）が特定されている反応であれば，3次元ドッキングのように反応側の情報を加味したアプローチも可能である．しかし，メカニズムやターゲットが解明されている毒性は非常に限られており，そうしたアプローチは利用出来ない．近年，（Q)SARと共に安全性評価の効率化の手段として期待されているのが*in vitro*評価系である．米国EPAが中心となって開始したToxCast（Tox21）プログラムでは，多数の*in vitro*ハイスループットアッセイと（Q)SARを組み合わせた毒性評価手法の構築を進めている[22]．毒性分野における*in vitro*評価系の多くは動物試験の代替法として開発される系が多いが，ToxCastにおける*in vitro*アッセイの多くは，創薬分野で用いられるメカニズムアッセイであり，個々のアッセイ結果は必ずしも直接毒性と結び付くものではなく，むしろ，毒性予測におけるパラメータとしての化学物質と生体の様々な相互作用反応を示すものと捉えることが出来る．一つの化学物質の安全性評価のために，ToxCastにおける*in vitro*アッセイを全て実施するのはコストや効率の面から現実的ではないが，数種の*in vitro*系により，化学構造からは計算出来ない重要なパラメータについてデータギャップを埋めることが可能であれば，（Q)SARと*in vitro*系を個別に用いるよりも，効率的かつ信頼出来る安全性評価ストラテジーが確立可能であろう．今後はそうした方向からの検討も進めていきたいと考えている．

参考文献

1）Matthews, E. J., and Contrera, J. F.: *Expert Opin Drug Metab Toxicol 3*, 125-34 (2007).
2）Cramer, G. M., Ford, R. A., and Hall, R. L.: *Food Cosmet Toxicol 16*, 255-76 (1978).
3）Munro, I. C., Ford, R. A., Kennepohl, E., and Sprenger, J. G.: *Food Chem. Toxicol. 34*, 829-67 (1996).
4）Renwick, A. G.: *Toxicol. Appl. Pharmacol. 207*, 585-91 (2005).
5）Abraham, M.: *Eur J Med Chem 37*, 595-605 (2002).
6）Zhu, C., Jiang, L., Chen, T., and Hwang, K.: *Eur J Med Chem* 37, 399-407 (2002).
7）http://qsar.cerij.or.jp/degacc/cgi-bin/index.cgi
8）http://kate.nies.go.jp/
9）Bennett, E. R., Clausen, J., Linkov, E., and Linkov, I.: *Chemosphere, 77*, 1412-8 (2009).
10）Wang, R., Fu, Y., and Lai, L.: *J Chem Inf Model*, American Chemical Society 37, 615-621 (1997).
11）Hayashi, M., Kamata, E., Hirose, A., Takahashi, M., Morita, T., and Ema, M.: *Mutat. Res. 588*, 129-35 (2005).
12）Greene, N., Judson, P. N., Langowski, J. J., and Marchant, C. A.: *SAR QSAR Environ Res 10*, 299-314 (1999).
13）Stuper, A. J., and Jurs, P. C.: *J Chem Inf Model 16*, 99-105 (1976).
14）Klopman, G.: *J Chem Inf Comput Sci 38*, 78-81 (1998).
15）Steinbeck, C., Hoppe, C., Kuhn, S., Floris, M., Guha, R., and Willighagen, E. L.: *Curr. Pharm. Des. 12*, 2111-20 (2006).
16）Frank, E., Hall, M., Trigg, L., Holmes, G., and Witten, I. H.: *Bioinformatics 20*, 2479-81 (2004).
17）Breiman, L.: *Mach Learn 45*, 5-32 (2001).
18）Hofer, H., Borgelt, C., and Berthold, M. R.: *Intelligent Data Analysis 8*. 495-504 (2004)
19）Zvinavashe, E., Murk, A. J., and Rietjens, I. M.: *Chem. Res. Toxicol. 21*, 2229-36 (2008).
20）van Leeuwen, K., Schultz, T. W., Henry, T., Diderich, B., and Veith, G. D.: *SAR QSAR Environ Res 20*, 207-20 (2009).
21）Matthews, E. J., Kruhlak, N. L., Benz, R. D., Contrera, J. F., Marchant, C. A., and Yang, C.: *Toxicol. Mech. Methods 18*, 189-206 (2008).
22）Dix, D. J., Houck, K. A., Martin, M. T., Richard, A. M., Setzer, R. W., and Kavlock, R. J.: *Toxicol. Sci. 95*, 5-12 (2007).

Bull. Natl. Inst. Health Sci., **128**, 27-28 (2010) **Special Report**

レギュラトリーサイエンスにおけるコンピュータを用いた構造活性予測研究の現状と展望

広瀬明彦

Researches on the *in silico* prediction of structure-activity relationship in the regulatory science sectors

Akihiko Hirose

Requirements of *in silico* toxicity prediction system are increasing in the chemical risk assessment fields, as well as in toxicity prediction at the early stage of the new drug development process. Recent amended chemical registration rules require internationally the risk assessment of huge amounts of existing chemicals. The (quantitative) structure-activity relationship ((Q)SAR) models are considered to be most effective tools for the acceleration of toxicity evaluation. In Europe or the United State, several research projects for the development of the (Q)SAR models are ongoing. Following this introduction, four researches on development of *in silico* prediction systems for (Q)SAR in the NIHS are reviewed. These activities must internationally contribute to the integrated chemical risk assessment approaches and/or could assist in the new drug development work.

Keywords: structure-activity relationship, in silico toxicity prediction, risk assessment

コンピュータを用いた（定量的）構造活性相関（(Q)SAR）モデルの発展は，近年のめざましいコンピュータ性能の進化と相俟って，大型コンピュータを必要とした複雑な計算を机上のパーソナルコンピュータで行うことを可能とすると共に，現実的でなかった生体分子の構造や医薬品などの化学物質との原子レベルでの相互作用を解析することが可能となるなど著しいものがある．これらコンピュータを用いた基盤的な（Q)SAR研究の進展は，基礎生物学的な生体反応の解明だけにとどまらず，応用的には特に創薬開発研究などへの貢献が期待されてきていた．一方，このような*in silico*技術は医薬品や環境化学物質と生体との相互作用により引き起こされる有害影響を説明することにも利用できることは明らかであり，近年，医薬品や化学物質の安全性評価を行う研究者や欧米の規制当局側においてリスク評価に有効的なツールとして利用するための試みが活発化してきている．

2007年より施行された欧州の化学品REACH規制（化学物質の登録，評価，許可，制限に関する規則）においては，それまでの既存化学物質や新規化学物質の区別を無くし，年間１トン以上製造または輸入される物質すべてについて登録が義務づけられ，製造・輸入量に応じて要求される毒性情報レベルは異なるものの，2018年までに約３万種といわれる既存化学物質の毒性情報を収集，評価することが求められている．しかし，数万種にも及ぶ化学物質すべてに対して要求される毒性試験を行うことは不可能であることは明らかであり，動物愛護の観点も考慮すると時間と費用を費やしてでも*in vivo*毒性試験を継続していくという選択も，社会的な理解を得ることは困難なところである．一方で，動物実験の代替法としての*in vitro*試験法を開発するための国際的な活動も近年活発化しているが，*in vivo*毒性試験よりスループットが高い*in vitro*試験をもってしても，数万種に及ぶ化合物の実測データを収集することは容易ではなく，しかも多様なエンドポイントをすべて代替するための*in vitro*試験の開発には，まだ相当の時間と技術の向上を必要としている段階である．そのため，類似構造に基づく共通の有害影響の可能性を推定することによるカテゴリーアプローチや（Q)SARモデルの適用は必須のものであると考えられている．欧州ではREACH規則への適用を目指した(Q)SAR研究プロジェクト（ToxTree[1],

To whom correspondence should be addressed:
Akihiko Hirose: 1-18-1 Kamiyoga, Setagaya-ku, Tokyo 158-8501, Japan; Tel: +81-3-3700-9878; Fax: +81-3-3700-1408; E-mail: hirose@nihs.go.jp

OpenTox[2], Caesar Project[3]）が進行しており，これらに市販のDEREKやMultiCASEなどのモデルも取り込んで，既存の毒性試験データベースを基にカテゴリー作成の支援を行うOECD QSAR application toolboxという統合化プラットフォームの開発もOECDのイニシアチブで進行している．米国では，大規模な*in vitro*試験データを基にした毒性予測システムの開発を目指したToxCastプロジェクト[4]などのcomputational toxicologyが進んでいるところである．本特論ではこのような国際的な動向に対応して，国立医薬品食品衛生研究所の４つの部を中心に行われている(Q)SAR研究を紹介する．これらは，現状ではまだ欧米プロジェクト等との直接的な連携は行われていないが，昨年の化審法改正にみられるレギュラトリー分野での国際化に向けて，今後レギュラトリー分野で最も注目される研究分野の一つとなることは疑う余地はない．

1 http://ecb.jrc.ec.europa.eu/qsar/qsar-tools,
2 http://www.opentox.org/,
3 http://www.caesar-project.eu,
4 http://epa.gov/ncct/toxcast/

Reproductive Toxicology 30 (2010) 343–352

Contents lists available at ScienceDirect

Reproductive Toxicology

journal homepage: www.elsevier.com/locate/reprotox

Review

Reproductive and developmental toxicity studies of manufactured nanomaterials

Makoto Ema*, Norihiro Kobayashi, Masato Naya, Sosuke Hanai, Junko Nakanishi

Research Institute of Science for Safety and Sustainability, National Institute of Advanced Science and Technology (AIST), 16-1 Onogawa, Tsukuba, Ibaraki 305-8569, Japan

ARTICLE INFO

Article history:
Received 4 December 2009
Received in revised form 27 April 2010
Accepted 16 June 2010
Available online 25 June 2010

Keywords:
Nanomaterials
Nanoparticles
Titanium dioxide
Fullerenes
Metallic particles
Luminescent particles
Reproductive and developmental toxicity
Testicular toxicity

ABSTRACT

This paper reviews studies *in vivo* and *in vitro* on the reproductive and developmental toxicity of manufactured nanomaterials including metallic and metal oxide-based particles, fullerenes (C_{60}), carbon black (CB), and luminescent particles. Studies *in vivo* showed increased allergic susceptibility in offspring of mouse dams intranasally insufflated with respirable-size titanium dioxide (TiO_2), adverse effects on spermatogenesis and histopathological changes in the testes and changes in gene expression in the brain of mouse offspring after maternal subcutaneous injection of TiO_2 nanoparticles, transfer to rat fetuses of radiolabeled gold nanoparticles and C_{60} after maternal intravenous injection, death and morphological abnormalities in mouse embryos after maternal intraperitoneal injection of C_{60}, and adverse effects on spermatogenesis in mouse offspring after maternal intratracheal instillation of CB nanoparticles. Studies *in vitro* revealed that TiO_2 and CB nanoparticles affected the viability of mouse Leydig cells, that gold nanoparticles reduced the motility of human sperm, that silver, aluminum, and molybdenum trioxide were toxic to mouse spermatogonia stem cells, that silica nanoparticles and C_{60} inhibited the differentiation of mouse embryonic stem cells and midbrain cells, respectively, and that cadmium selenium-core quantum dots inhibited pre- and postimplantation development of mouse embryos. Although this paper provides initial information on the potential reproductive and developmental toxicity of manufactured nanomaterials, further studies, especially *in vivo*, using characterized nanoparticles, relevant routes of administration, and doses closely reflecting expected levels of exposure are needed.

Contents

* Corresponding author. Tel.: +81 29 861 8021; fax: +81 29 861 8338.
E-mail address: ema-makoto@aist.go.jp (M. Ema).

0890-6238/$ – see front matter © 2010 Elsevier Inc. All rights reserved.
doi:10.1016/j.reprotox.2010.06.002

1. Introduction

Nanomaterials are defined as materials having a physicochemical structure on a scale greater than typical atomic/molecular dimensions but less than 100 nm (nanostructure), which exhibit physical, chemical and/or biological characteristics associated with a nanostructure [1]. Nanoparticles are defined as particles with at least one dimension smaller than 100 nm and include manufactured nanoparticles, ambient ultrafine particles and biological nanoparticles [1,2]. Humans have been exposed to airborne nanoparticles throughout evolution, but exposure has increased dramatically because of anthropogenic factors including combustion engines, power plants, and other sources of thermodegradation [2]. The rapidly developing field of nanotechnology, which is creating materials with size-dependent properties, is likely to become another source of exposure to nanomaterials. The surface and interface of particles are particularly important components of nanoparticles. Nanomaterials have an increased surface area: mass ratio thereby greatly enhancing their chemical/catalytic reactivity compared to normal-sized forms of the same substance. Surface coatings can be utilized to alter surface properties of nanoparticles to prevent aggregation or agglomeration with different particle-types, and/or serve to passivate the particle-type to migrate the effects of ultraviolet radiation-induced reactive oxidants [1]. The distinctive and often unique properties of nanomaterials offer the promise of broad advances for a wide range of technologies. Nanomaterials are used in a variety of areas including advanced materials, electronics, magnetics and optoelectronics, biomedicine, pharmaceuticals, cosmetics, energy, and catalytic and environmental detection and monitoring [3,4]. At present, there are relatively few environments where exposures are known to occur. However, if the commercialization of products using nanomaterials develops as anticipated, the potential for exposure is likely to increase notably over the coming decade [1]. Despite growing concern over the possible risk that nanomaterials pose, there is a lack of information on their potential toxicity. At this moment, there is a knowledge gap between the increasing development and use of nanomaterials and the prediction of possible health risks.

In recent years, reproductive and developmental toxicity has increasingly become recognized as an important part of overall toxicology. In fact, adverse effects of environmental chemicals on the reproductive success of wildlife populations have been noted [5]. It is reported that nanoparticles can pass through biological membranes [6,7]; raising fears that they can affect the physiology of any cell in the body. The possibility of chemicals entering biological systems is of great concern to the public with regard to possible reproductive and developmental toxicity. In this paper, we review studies on the reproductive and developmental toxicity of nanomaterials, published in openly available scientific literature.

2. Reproductive and developmental toxicity of manufactured nanomaterials

The literature on manufactured nanomaterials was searched using TOXNET/TOXLINE for studies *in vivo* and *in vitro* of reproductive and developmental toxicity, excluding abstracts. Although no information was available on the reproductive and developmental toxicity of single- or multi-wall carbon nanotubes, articles on metallic and metal oxide-based particles, fullerenes (C_{60}), and carbon black (CB) and luminescent particles were found. In this paper, we review studies using mammalian animals and cells on the reproductive and developmental effects of nanomaterials. The final search of the literature was conducted in March, 2010.

2.1. Metallic and metal oxide-based particles

In vivo and *in vitro* studies of titanium dioxide (TiO_2) nanoparticles, and *in vitro* studies of silver, aluminum, molybdenum trioxide (MoO_3), gold, magnetic iron oxide (Fe_3O_4), cobalt–chromium (CoCr) and silica nanoparticles have been published.

2.1.1. Titanium dioxide (TiO_2)

TiO_2 is widely used as a white pigment in paints, plastics, inks, paper, creams, cosmetics, drugs and foods. TiO_2 was previously classified as biologically inert in animals and humans [8–10] and has been used as a negative control particle in a variety of toxicological studies. Recently, concern has been raised on possible adverse effects of TiO_2 on human health because exposure to high concentrations of ultrafine TiO_2 was involved in the induction of lung inflammatory responses [11] and tumors [12]. Very recently, the International Agency for Research on Cancer (IARC) Monograph Working Group classified TiO_2 as possibly carcinogenic to humans (i.e., group 2B) based on results from studies in which the inhalation and intratracheal instillation of TiO_2 provided sufficient evidence in animals for carcinogenicity [13]. As for genotoxicity, the results of studies on TiO_2 nanoparticles are inconclusive [14,15]. *In vivo* and *in vitro* studies of TiO_2 are summarized in Table 1.

2.1.1.1. In vivo study of titanium dioxide (TiO_2). Pregnant BALB/c mice on gestational day (GD) 14 or nonpregnant control mice were administered respirable-size TiO_2 [16], that is less than 10 μm in particle size [17], suspended in phosphate-buffered saline (PBS) at 50 μg/mouse by a single intranasal insufflation. Pups obtained by spontaneous delivery received a single intraperitoneal injection of ovalbumin (OVA) with alum on postnatal day (PND) 4. These pups were exposed to aerosolized OVA on PNDs 12–14, and subjected to an examination of pulmonary function and a pathological analysis. Airway responsiveness to increasing concentrations of aerosolized methacholine was measured using whole body plethysmography. Bronchoalveolar lavage (BAL) differential cell counts and histopathological examinations of the lung were also performed. Lung inflammatory responses were determined 48 h postadministration in nonpregnant and pregnant mice ($n > 9$/group). TiO_2-treated nonpregnant mice exhibited minimal increases in BAL polymorphonuclear leukocyte counts, whereas pregnant mice showed acute neutrophilic inflammation. Pregnant mice exposed to TiO_2 had higher serum levels of cytokines, including interleukin-1β, tumor necrosis factor-α, interleukin-6 and chemokine, 48 h after exposure compared with nonpregnant mice ($n = 9$/group). Offspring of dams exposed to TiO_2 showed increased airway hyperresponsiveness, increased percentage of eosinophils, and pulmonary inflammation ($n = 17$–21/group). These findings indicate that TiO_2 caused acute cellular inflammation in pregnant mice and increased allergic susceptibility in their pups.

A TiO_2 nanopowder (25–70 nm in particle size, 20–25 m^2/g in surface area, anatase, Sigma–Aldrich Japan, Inc.) suspended in saline with 0.05% Tween 80 was subcutaneously injected into pregnant Slc:ICR mice ($n = 15$) on GDs 6, 9, 12 and 15 at

Table 1
In vivo and *in vitro* reproductive and developmental toxicity studies of titanium dioxide (TiO_2) particles.

In vivo/*in vitro*	Materials/characteristics	Animals/cells	Exposure			Findings	References
			Route/method	Duration/time	Dose/concentration		
In vivo	Respirable-size	BALB/c mice	Intranasal insufflation	Single on GD 14	50 μg/mouse	↑ Acute cellular inflammation in pregnant mice ↑ Susceptibility to allergy in pups	[16]
In vivo	25–70 nm in particle size, 20–25 m^2/g in surface area, anatase	Slc:ICR mice	Subcutaneous injection	GDs 6, 9, 12, and 15	100 μg/mouse/day (14–15 mice/group)	Changes in gene expression related to development and function of central nervous system in male pups	[18]
In vivo	25–70 nm in particle size, 20–25 m^2/g in surface area, anatase	Slc:ICR mice	Subcutaneous injection	GDs 3, 7, 10, and 14	100 μg/mouse/day (6 mice/group)	↓ Body weight of pups ↓ DSP of pups ↓ Epididymal sperm motility in pups ↓ Number of Sertoli cells in pups Histopathological changes in testis of pups	[19]
In vitro	25–70 nm in particle size	Mouse testis Leydig cell line TM3	Incubation	16, 24, or 48 h	1–1000 μg/mL	↓ Viability of TM3 at 100 μg/mL ↓ Proliferation of TM3 cells at 100 μg/mL No changes in HO-1 or StAR mRNA expression at up to 100 μg/mL	[20]

100 μg/mouse/day as the exposure group, and 100 μl of vehicle alone was injected into pregnant mice ($n = 14$) as the control group [18]. Brain tissue was obtained from male offspring on embryonic day 16 ($n = 8$/group) or on PND 2 ($n = 10$/group), PND 7 ($n = 10$/group), or PND 21 ($n = 9$/group), total RNA was extracted from whole brain, and gene expression was analyzed. Maternal exposure to TiO_2 caused changes in the expression of genes associated with brain development, cell death, response to oxidative stress, and mitochondria in the brain during the prenatal period, and genes associated with inflammation and neurotransmitters in the later stages. However, this study did not investigate how maternal behavior toward the pups changed and how this in turn altered gene expression. It is difficult to evaluate the change in gene expression using the toxicogenomic data of this study, because not enough microarray data was provided in the paper.

Slc:ICR mice ($n = 6$/group) were subcutaneously injected with TiO_2 nanoparticles (25–70 nm in particle size, 20–25 m^2/g in surface area, anatase, Sigma–Aldrich) suspended in saline with 0.05% Tween 80 at 100 μg/mouse/day on GDs 3, 7, 10 and 14 [19]. Male offspring were autopsied on PND 4 or postnatal week (PNW) 6. Lower body weights were found among offspring of dams exposed to TiO_2. Aggregates of TiO_2 nanoparticles (100–200 nm) were detected in Leydig cells, Sertoli cells, and spermatids in the testes of pups on PND 4 and PNW 6. Disorganized and disrupted seminiferous tubules, tubule lumens with few mature sperm, and decreases in daily sperm production (DSP), epididymal sperm motility, and numbers of Sertoli cells were observed at PNW 6 in pups of the TiO_2-treated group ($n = 8$/group). TiO_2 particles were detected in cells of the olfactory bulb and cerebral cortex of pups at PNW 6. There were many cells positive for caspase-3, an enzymatic marker of apoptosis, in the olfactory bulb of pups on PNW 6 in the TiO_2-exposed group. Although the possibility of adverse effects of TiO_2 nanoparticles on brain development is noted, the behavioral effects of nanoparticles were not investigated. There was a lack of description on the maternal findings in this report.

2.1.1.2. In vitro study of titanium dioxide (TiO_2). The direct effects of TiO_2 (25–70 nm in particle size, Aldrich) on testis-constituent cells was determined using the mouse Leydig cell line TM3, testosterone-producing cells of the testis [20]. TiO_2 was suspended in a balanced salt solution [0.05% Tween 80–0.25% DMSO in PBS(−)], and sonicated for 10 min immediately prior to use in the assay. TiO_2 was added to the culture system for 16, 24, or 48 h. The uptake of TiO_2 nanoparticles by Leydig cells was detected after incubation of cells with TiO_2 at 30 μg/mL for 48 h. Following incubation of cells with TiO_2 at 10 or 100 μg/mL, a remarkable inhibition of viability and transient reduction in proliferation of TM3 cells were observed at 100 μg/mL after 24 h. No effect of TiO_2 was found on the expression of heme oxygenase-1 (HO-1), a sensitive marker of oxidative stress, or steroidogenic acute regulatory (StAR) mRNA in TM3 cells treated for 16 h at up to 100 μg/mL or for 48 h at up to 30 μg/mL. These findings suggest that TiO_2 nanoparticles have no direct effect on the induction of oxidative stress or synthesis of testosterone in Leydig cells.

2.1.2. Gold

Colloidal gold has been used in medical applications and gold nanoparticles are used commercially in a wide array of catalytic applications and optical and electrical applications as components of various probes, sensors, and optical devices [21]. *In vivo* and *in vitro* studies of gold particles are shown in Table 2.

2.1.2.1. In vivo study of gold. The distribution of ^{198}Au-colloidal particles (4–200 nm) was determined after a single injection into the iliac artery of pregnant SD rats on GDs 16–18 [22]. Although more than 90% of the radiocolloid was found in the maternal liver

Table 2
In vivo and *in vitro* reproductive and developmental toxicity studies of gold particles.

In vivo/*in vitro*	Materials/characteristics	Animals/Cells	Exposure			Findings	References
			Route/method	Duration/time	Dose/concentration		
In vivo	^{198}Au-colloidal particles (4–200 nm in diameter)	SD rats	Intraarterial injection	Single during GDs 16–18	200 μL/rat	No detection of radioactivity in amniotic fluid, fetal membranes, or fetus	[22]
In vivo	^{198}Au-colloidal nanoparticles (5 or 30 nm in diameter)	Wistar rats	Intravenous injection	Single on GD 19	0.5 mL/rat of solution contained 20 μg of gold (7–10 rats/group)	Transfer rate to fetus: 0.018% for 5 nm particles Transfer rate to fetus: 0.005% for 30 nm particles	[23]
In vivo	Colloidal gold nanoparticles (2 or 40 nm in diameter)	C57BL/6 mice	Intravenous injection	On GDs 16–18	1 mL/rat of solution contained gold particle (5 mice/group)	No transfer to fetus	[24]
In vitro	Gold nanoparticles (10, 15, or 30 nm in diameter) coated with polyethylene glycol	Human placenta	Open perfusion	5 min	7.9×10^{11} for 15 nm particles and 7.8×10^{10} for 30 nm particles	Detection of high levels of nanoparticles soon after perfusion in maternal outflow No detection of nanoparticles in fetal outflow	[25]
In vitro	Gold nanoparticles (10, 15, or 30 nm in diameter) coated with polyethylene glycol	Human placenta	Recirculating perfusion	6 h	9.1×10^{9} for 10 nm particles and 2.0×10^{9} for 15 nm particles	No transplacental transfer of nanoparticles	[25]
In vitro	Gold nanoparticles (9 nm in size)	Human sperm	Mixed with semen		44 ppm	↓ Sperm motility	[26]

at 15 min after injection, no radioactivity was detected in the amniotic fluid, fetal membranes, or fetus. These findings indicate the impermeability of the rat placenta to colloidal gold. Detailed experimental conditions including concentrations of gold particles and numbers of rats used were not described in this report.

Pregnant Wistar rats (n = 7–10/group) were injected intravenously with ^{198}Au-colloidal particles (5 and 30 nm in diameter, Daichi Radio Isotope Co., Ltd. and Hoext Japan Co., Ltd., respectively) into the tail vein on GD 19 (vaginal plug = GD 1) and sacrificed 1 or 24 h later [23]. The 0.5 mL of solution injected contained 20 μg of gold. The clearance of ^{198}Au-colloid from blood was faster in dams injected with the 30 nm particles than in dams injected with the 5 nm particles, and, therefore, the radioactivity remaining in maternal blood was greater in the 5 nm-group. Fetal radioactivity was detected in pregnant rats sacrificed at 1 and 24 h after the injection of 5 nm particles and at 24 h after the injection of 30 nm particles. The transfer rate to the fetus was very small, being approximately 0.018 and 0.005% for the 5 and 30 nm particles, respectively. The levels of radioactivity in the fetal membrane and placenta were greater in the 5 nm-group that in 30 nm-group, and 100–300 times greater than the levels in the fetus for either group. The authors described that the transfer or deposition of ^{198}Au-colloid was directly affected not by particle size, but by the average concentration in maternal blood.

Pregnant C57BL/6 mice were intravenously injected into the tail vein with 1 mL of a solution containing 2 or 40 nm colloidal gold nanoparticles (n = 5/goroup) or 1 mL of saline (n = 3 as controls) on GDs 16–18 and killed 24 h after the last injection [24]. The 2 and 40 nm gold nanoparticles (Fitzgerald Industry Inc.) contained 15×10^{13} particles (12.13 μg) and 9×10^{10} particles (58.21 μg), respectively. The gold nanoparticles had a negative surface charge and were monodispers and spherical in shape. No particles were detected in the fetuses and placentae. These findings suggest that gold nanoparticles do not penetrate the placental barrier.

2.1.2.2. In vitro study of gold. The transplacental transfer of monodispersed gold particles (10, 15, and 30 nm in diameter before coating) coated with polyethylene glycol (PEG) was examined using placentae from healthy, nonsmoking mothers [25]. In the open perfusion as a "once-through" perfusion, nanoparticles (7.9×10^{11} for 15 nm particles and 7.8×10^{10} for 30 nm particles) were suspended in 5 mL of physiological saline and injected into the maternal artery within 5 min, and the maternal and fetal outflow were collected at 3-min intervals for 18 min. In the maternal outflow, the nanoparticles of 15 and 30 nm were detected at 570 and 678 ppb within 3–6 min of injection, and only 9.3 and 18.0 ppb, respectively, at the end of perfusion. No nanoparticles were detected in the fetal outflow. Recirculating perfusion was performed with 10 and 15 nm nanoparticles only. Both the maternal and fetal sides were recirculated. The nanoparticles (9.1×10^{9} for 10 nm particles and 2.0×10^{9} for 15 nm particles) were added to the maternal reservoir and the perfusion was continued for 6 h. Samples were taken from the maternal and fetal reservoirs every 30 min for the first 2 h, and once per hour thereafter. Nanoparticles did not cross the placenta regardless of particle size. At the end of the perfusion, concentrations of nanoparticles in maternal perfusate samples decreased 41 and 64% giving final concentrations of 24.2 and 22.2 ppb for the 10 and 15 nm nanoparticles, respectively. The gold aggregates were located in syncytiotrophoblasts and trophoblasts, but no gold particles were detected in the fetal capillary endothelium in perfused tissue. These findings indicate that PEGylayed gold nanoparticles do not cross the human placenta from the maternal to fetal circulation.

The effect of gold nanoparticles (9 nm) at a concentration of 44 ppm on human sperm was determined using a single, fresh, donor semen sample from a healthy male [26]. In a mixture of 500 μL of the gold nanoparticle solution and semen, 25% of sperm

were not motile. The rate of motility among the control sperm was 95%. The penetration of sperm heads and tails by gold nanoparticles, and fragmentation of sperm were found in the mixture. Toxicity parameters, except for motility, were not investigated in this study.

2.1.3. Silver, aluminum, and molybdenum trioxide (MoO_3)

Nanoscaled silver powder is used in biocides, transparent conductive inks and pastes, and various consumer and industrial products that need enhanced antimicrobial properties [21]. Nanoscaled aluminum powder is used in various electronic circuits and as a scratch-resistant coating for plastic lenses, antimicrobial agents, and new tissue-biopsy tools [21]. MoO_3 nanoparticles have electrochromic, photochromic, and gas-sensing properties [27]. *In vitro* studies of silver, aluminum, and MoO_3 particles are listed in Table 3.

2.1.3.1. In vitro study of silver, aluminum, and molybdenum trioxide (MoO_3). *In vitro* studies of silver (15 nm in diameter), aluminum (30 nm in diameter), and MoO_3 (30 nm in diameter) nanoparticles were performed using the C18-4 cell line, which was established from type A spermatogonia isolated from 6-day-old mouse testes [28]. The cells were immortalized and exhibited phenotypic characteristics of germline stem cells *in vivo*, were adherent, and responded to the growth factor glial cell line-derived neurotrophic factor. Nanoparticles were dispersed in PBS at final concentrations of 5, 10, 25, 50, and 100 μg/mL culture medium, and the C18-4 cells were incubated with nanoparticles for 48 h. Silver nanoparticles caused necrosis and apoptosis at 10 μg/mL and above. Aluminum nanoparticles did not induce shrinkage, necrosis, or apoptosis below 10 μg/mL. No distinct changes in cell morphology were observed at any concentration of MoO_3 nanoparticles. Reduced mitochondrial function and cell viability were noted after incubation with silver nanoparticles at 10 μg/mL, and the EC_{50} was calculated at 7.75 μg/mL. The effects of aluminum nanoparticles on mitochondrial function could not be determined because the particles accumulated in the cells and formed cytoplasmic aggregates at low concentrations. MoO_3 nanoparticles reduced mitochondrial function at 50 μg/mL and above, and the EC_{50} was 90 μg/mL. Silver nanoparticles slightly increased lactase dehydrogenase (LDH) leakage at 5 μg/mL, and the EC_{50} was 2.5 μg/mL. The leakage of LDH was increased by aluminum nanoparticles at 5 μg/mL and above, values reaching a plateau at around 25 μg/mL and the EC_{50} being 4.7 μg/mL. An increase in LDH leakage was observed with MoO_3 nanoparticles at 5 μg/mL and above, and the value reached a plateau at 10 μg/mL. The EC_{50} was 5 μg/mL. An increased number of apoptotic C18-4 cells were found after incubation with silver nanoparticles at 5 μg/mL, aluminum nanoparticles at 5 and 10 μg/mL, and MoO_3 nanoparticles at 50 μg/mL. These results indicate that silver nanoparticles are most toxic and MoO_3 nanoparticles are least toxic to this cell line. The authors noted that this cell line provides a valuable model to assess the cytotoxicity of nanoparticles in the germ line *in vitro*.

2.1.4. Magnetic iron oxide (Fe_3O_4)

The magnetic properties of magnetic iron oxide nanoparticles may lead to a range of new biomedical and diagnostic applications including cellular therapy by cell labeling and targeting, tissue repair, drug delivery, magnetic resonance imaging, and magnetofection [29]. An *in vivo* study of magnetic Fe_3O_4 particles is presented in Table 3.

2.1.4.1. In vitro study of magnetic iron oxide (Fe_3O_4). The effect of Fe_3O_4 on sperm was determined after incubation of bovine sperm in glucose-free modified Tyrode solution with an aqueous colloid solution of Fe_3O_4 nanoparticles coated with poly(vinyl alcohol) for 2 h at 37 °C [29]. The final concentration of Fe ions was 7.35 mM. In

Table 3
In vitro reproductive and developmental toxicity studies of silver, aluminum, molybdenum trioxide (MoO_3), magnetic iron oxide (Fe_3O_4), cobalt–chromium (CoCr) and silica (SiO_2) particles.

Materials/characteristics	Cells	Exposure			Findings	References
		Route/method	Duration/time	Dose/concentration		
Silver nanoparticles (15 nm in diameter)	Mouse spermatogonia stem cell line C18-4	Incubation	48 h	5–100 μg/mL	↑ Necrosis and apoptosis at 10 μg/mL and above ↓ Mitochondrial function and cell viability at 10 μg/mL ↑ LDH leakage at 5 μg/mL ↑ Apoptotic cells at 5 μg/mL	[28]
Aluminum nanoparticles (30 nm in diameter)	Mouse spermatogonia stem cell line C18-4	Incubation	48 h	5–100 μg/mL	No shrinkage, necrosis, or apoptosis of cells at below 10 μg/mL ↑ LDH leakage at 5 μg/mL ↑ Apoptotic cells at 5 and 10 μg/mL	[28]
MoO_3 nanoparticles (30 nm in diameter)	Mouse spermatogonia stem cell line C18-4	Incubation	48 h	5–100 μg/mL	No distinct change in cell morphology ↓ Mitochondrial function at 50 μg/mL and above ↑ LDH leakage at 5 μg/mL ↑ Apoptotic cells at 50 μg/mL	[28]
Magnetic Fe_3O_4 nanoparticles coated with poly(vinyl alcohol)	Bovine sperm	Incubation	6 h	7.35 mM (as Fe ions)	No adverse effect on sperm motility or acrosome reaction	[29]
CoCr nanoparticles (29.5 nm in diameter)	Human trophoblast choriocarcinoma cell line and Layer of BeWo b30 cells	Direct and indirect exposure	24 h	0.036 mg/cm^2	↑ DNA damage of fibroblasts by indirect exposure	[30]
Spherical amorphous silica nanoparticles (10, 30, 80, or 400 nm in average primary particle size)	D3 murine embryonic stem cell line	Incubation	10 days	1–100 μg/mL	↓ Differentiation of embryonic stem cells after exposure to 10 and 30 nm, but not 80 and 400 nm, particles	[32]

the first 20 min of incubation, 23% of the particles were taken up by sperm cells. Later on, about 60% of these particles were released from the cells and a further linear uptake was observed for an additional 1.5 h of incubation. Particles were bound to the acrosome in the head of the sperm, and to mitochondria in the tail of the sperm. The sperm was further incubated for 4 h. Motility and the ability to undergo an acrosome reaction, i.e. the ability to fertilize an egg, were not affected by the presence of the magnetic nanoparticles.

2.1.5. Cobalt–chromium (CoCr) nanoparticles

Internal exposure to CoCr nanoparticles can occur by wear mechanism associated with metal-on-metal (CoCr) orthopaedic joint replacements [30]. An *in vitro* study of CoCr particles is presented in Table 3.

2.1.5.1. In vitro study of cobalt–chromium (CoCr) nanoparticles. The cellular toxicity of CoCr nanoparticles (29.5 ± 6.3 nm in diameter, Osprey Metals) when located on the other side of a fully confluent cellular barrier was assessed using BeWo b30 cells, a human trophoblast choriocarcinoma-derived cell line, which were grown as a multi-layered (3–4 cells thick) barrier to simulate tight barriers in the body like the placental barrier [30]. Human fibroblast cells were placed on one side of this layer of cells, and CoCr particles on the other. The fibroblasts were checked for DNA damage using the alkaline comet assay after introduction of the particles. Indirect exposure to CoCr nanoparticles caused DNA damage. Indirect exposure to micrometer-sized CoCr (2.9 ± 1.1 μm in diameter) also damaged DNA. More than 95% of the nanoparticles were located within the cells of the superficial layer after 24 h of exposure, indicating that nanoparticles were internalized by the BeWo cells and did not pass through the barrier. The authors of this paper noted that the DNA damage was mediated by a novel mechanism involving pannexin and connexin hemichannels and gap junctions and purinergic signaling. These findings suggest that there is some possibility of placental transfer of particles.

2.1.6. Silica (SiO_2)

Industrial silica products are widely used in the electronics industry and as a food additive, and nanosized amorphous silica is used in a wide variety of applications including catalytic supports, photonic crystals, gene delivery, photodynamic therapy, and biomedical imaging [31]. An *in vitro* study of silica particles is presented in Table 3.

2.1.6.1. In vitro study of silica (SiO_2). The embryonic stem (ES) cell test using the D3 murine ES cell line was performed to determine the potential of spherical amorphous silica nanoparticles (10, 30, 80 and 400 nm in average primary particle size, Glantreo Ltd.) to inhibit the differentiation of ES cells into spontaneously contracting cardiomyocytes [32]. Silica nanoparticles were dialyzed against pure MilliQ water and diluted in distilled water, and the ES cells were exposed at 1–100 μg/mL throughout the entire 10-day test period. Transmission electron microscopy revealed that the dried silica particles were spherical and showed no substantial aggregation, except for the 10 nm particles, and measured diameters of the particles specified as 10, 30, 80, and 400 nm by the manufacturer were 11, 34, 34, and 248 nm, respectively. Silica particles of 30, 80 and 400 nm were observed in cells of the embryonic body. A concentration-dependent inhibition of the differentiation of ES cells into contracting cardiomyocytes was observed after exposure to 10 and 30 nm particles while the 80 and 400 nm particles did not inhibit the differentiation at up to 100 μg/mL. The inhibitory effect of the 30 nm particles was greater than that of the 10 nm particles as evidenced by the estimated ID_{50} values, 29 and 59 μg/mL, respectively. Inhibition of the differentiation of ES cells occurred below cytotoxic concentrations, suggesting a specific effect of the 10 and 30 nm particles on the differentiation of the ES cells.

2.2. Fullerenes (C_{60})

A fullerene is any molecule entirely in the form of a hollow sphere, ellipsoid, or tube. The first fullerene to be discovered is known as buckminsterfullerene C_{60}. Fullerenes have unique physicochemical properties that have been exploited for use in cosmetics, lubricants, dietary supplements, building materials, clothing treatment, electronics, and fuel cells [33]. *In vivo* and *in vitro* studies on fullerenes are listed in Table 4.

2.2.1. In vivo study of fullerenes (C_{60})

[60]Fullerene (C_{60}, purity > 99.9%, Terms Co.) was solubilized with poly(vinylpyrrolidone) (PVP). Pregnant Slc mice (n = 2/group) were intraperitoneally injected with C_{60} at 25, 50, or 137 mg/kg, PVP, or distilled water on DG 10, and their embryos were examined 18 h after injection [34]. No effects were observed in embryos of dams injected with PVP or distilled water. After the injection of C_{60}, all embryos died at 137 mg/kg. At 50 mg/kg, C_{60} was clearly distributed into the yolk sac and embryos and 50% of embryos were abnormal in shape predominantly in the head and tail regions. At 25 mg/kg, one pregnant mouse had all normal embryos and the other had only one abnormal embryo. The authors of this study speculated that C_{60} was incorporated into the concepts and the severely disrupted the function of the yolk sac and embryonic morphogenesis.

The distribution of $[^{14}C]_{60}$ was determined in rat dams and their pre- and postnatal offspring [35]. C_{60}, with an average particle size of less than 10 nm and estimated at 2 nm, was suspended in PVP. SD rats were given an intravenous injection of a suspension of approximately 0.3 mg $[^{14}C]_{60}$/kg into the tail vein on GD 15 or lactational day (LD) 8, and tissues of dams were collected 24 h (n = 4) and 48 h (n = 3) later. In pregnant dams at 24 h after injection, radioactivity was found in the liver (43% of the injected radioactivity), spleen (4%), reproductive tract (3%), and placenta (2%). Radioactivity was also detected in the digest of fetuses (0.87%). In lactating dams, radioactivity was detected in the liver (35%), spleen (4%), reproductive tract (0.10–0.42%), mammary tissue (0.48–0.94%), and milk at 24 h after injection. Radioactivity transferred to pups via lactation was found in the gastrointestinal tract (0.28%) in pups sacrificed at 24 h after injection, with an increase in distribution to the gastrointestinal tract of pups (0.43%) by 48 h after injection. The authors of this study noted that C_{60} distributed to the placenta and fetuses of exposed pregnant dams and to the milk and pups of exposed lactating dams.

2.2.2. In vitro study of fullerenes (C_{60})

Midbrain tissue samples of embryos of pregnant Slc–ICR mice on GD 11 were dissociated into individual cells, cell suspensions were prepared in culture medium, and a midbrain micromass culture was performed to evaluate the toxicity of C_{60} solubilized with PVP [34]. The C_{60} solution in the medium was incorporated into the midbrain culture plates, and further cultured for 6 days. The IC_{50} values of C_{60} for cell differentiation and proliferation were 0.43 and 0.47 mg/mL, respectively. Differentiation was inhibited as cytotoxicity increased. C_{60} was assumed to decrease cell proliferation via active oxygen species, because cell proliferation inhibited by C_{60} was partly restored by the addition of antioxidative enzymes.

2.3. Carbon black (CB)

CB is a low solubility particle produced industrially from incomplete thermal decomposition of hydrocarbons, a process controlled

Table 4
In vivo and *in vitro* reproductive and developmental toxicity studies of fullerenes (C_{60}), carbon black (CB), cadmium selenium-core quantum dots (CdSeQDs) and polystyrene-based fluorescent particles.

In vivo/*in vitro*	Materials/characteristics	Animals/cells	Exposure			Findings	References
			Route/method	Duration/time	Concentration		
In vivo	C_{60} (purity > 99.9%)	Slc mice	Intraperitoneal injection	Single on GD 10	25–137 mg/kg	Deaths of all embryos at 138 mg/kg Abnormalities in 50% of embryos at 50 mg/kg	[34]
In vivo	[^{14}C]C_{60} (>10 nm, estimated 2 nm in particle size)	SD rats	Intravenous injection	Single on DG 15 or LD 8	Approx. 0.3 mg/kg (3–4 rats/group)	Distribution of C_{60} to placentae and fetuses of exposed pregnant dams Distribution of C_{60} to milk and offspring of exposed lactating dams	[35]
In vitro	C_{60} (purity > 99.9%)	Midbrain cells of Slc:ICR mouse embryos at GD 11	Incubation	6 days	10–1000 μg/mL	IC_{50} for cell differentiation = 430 μg/mL IC_{50} for cell proliferation = 470 μg/mL	[34]
In vivo	CB Printex 90 (14 nm in particle size, 300 m^2/g in surface area) Printex 25 (56 nm in particle size, 45 m^2/g in surface area) Flammruss 101 (95 nm in particle size, 20 m^2/g in surface area)	ICR mice	Intratracheal instillation	10 times at weekly intervals	0.1 mg/mouse	No effect of 14, 56 or 95 nm particles on body weight or reproductive organs ↑ Serum testosterone levels after instillation of 14 and 56 nm particles ↓ DSP after instillation of 14, 56, and 90 nm particles	[37]
In vitro	CB (14 nm in particle size, Printex 90)	Mouse testis Leydig cell line TM3	Incubation	16, 24, or 48 h	1–1000 μg/mL	↓ Viability of TM3 at 1000 μg/ml No effect on proliferation of TM3 cells No changes in HO-1 mRNA expression at up to 100 μg/mL ↑ StAR mRNA expression at 30 μg/mL for 48 h-incubation	[20]
In vitro	CdSeQDs (approx. 3.5 nm in diameter) ZnS coating CdSeQDs	ICR mouse morulas and blastocysts	Incubation	24 h	125, 250, or 500 nmol/L	↓ Development of morulas into blastocysts at 250 and 500 nmol/L ↑ Number of apoptotic cells of blastocysts at 250 and 500 nmol/L ↓ Cell proliferation of blastocysts at 250 and 500 nmol/L ↓ Blastocyst development at 125 nmol/L and higher No cytotoxicity of ZnS coating CdSeQDs	[38]
In vitro	CdSeQDs (approx. 3.5 nm in diameter)	Female ICR and male C57BL/6J mice	Blastocysts were preincubated with CdSeQDs and transfered to pseudopregnat mice	Preincubation of blastocysts for 24 h	500 nmol/L	↓ Implantation rate ↑ Resorptions ↑ Embryos with abnormal development ↓ Fetal weight	[38]
In vitro	Polystyrene-based fluorescent nanoparticles (microspheres 40 to over 120 nm in size, Molecular Probes Inc.)	Two-cell stage mouse embryos	Incubation	4 days for 2-cell embryos 48 h for blastocysts	11.0 million/mL	No effect on development of 2-cell embryos No effect on hatching, implantation, or degeneration after exposure up to the blastocyst stage	[41]

to achieve pre-defined and reproducible particle sizes and properties suitable for a diverse range of industrial applications [36]. The CB particles so formed are complex, with a degenerated graphitic crystallite structure and high-power electron micrographs clearly show irregular layered graphitic plates. The most common use of CB is as a pigment and reinforcing phase in automobile tires. CB helps conduct heat away from the tread and belt area of the tire, reducing thermal damage and increasing tire life. CB is also employed in some radar-absorbent materials and in photocopiers and laser printer toner. *In vivo* and *in vitro* studies of CB are listed in Table 4.

2.3.1. In vivo study of carbon black (CB)

The effect of CB nanoparticles with a primary size of 14 nm ($300\ m^2/g$ in surface area, Printex 90, Degussa), 56 nm ($45\ m^2/g$ in surface area, Printex 25, Degussa), and 95 nm ($20\ m^2/g$ in surface area, Flammruss 101, Degussa) on the male reproductive system was determined [37]. Six-week-old male ICR mice ($n = 15–16$/group) were intratracheally instilled with CB particles suspended in normal saline containing 0.05% Tween 80 at 0.1 mg/mouse for the 14, 56, and 95 nm CB particles and 1.56 μg/mouse for the 14 nm CB (particle number concentration of 14 nm CB is the same as that of 56 nm CB). Mice received 10 weekly instillations and were killed on day after the last instillation. No effect of the 14, 56, or 96 nm particles was observed on body weight or male reproductive organ weights. Vacuolation of the seminiferous tubules and decreased DSP were found in mice instilled with all three sizes of CB particles. Levels of serum testosterone were increased after instillation of all three particles. The group exposed to the 14 nm particles, with approximately the same number of particles per unit volume as the 56 nm particles, showed fewer effects than did the group exposed to the 56 nm particles. The authors noted that CB nanoparticles impaired the function of Leydig cells, and the consequent fluctuation of sperm testosterone levels caused a reduction of DSP. These findings suggest that CB nanoparticles adversely affect mouse spermatogenesis and the effect depends on particle mass rather than particle number.

2.3.2. In vitro study of carbon black (CB)

The direct effects of CB (14 nm in particle size, Printex 90, Degussa) on testis-constituent cells was determined using the mouse Leydig cell line TM3 [20]. The test was performed using the procedure described above in the TiO_2 section. The uptake of CB nanoparticles by Leydig cells was detected after 48 h. Cell viability was markedly inhibited at 1000 μg/mL, but CB did not affect the proliferation of TM3 cells. No effect of CB was found on the expression of HO-1 mRNA in TM3 cells at up to 100 μg/mL. StAR mRNA expression was increased at 30 μg/mL after incubation for 48 h. These findings suggest that CB nanoparticles have no direct effect on the induction of oxidative stress but affect the production of steroid hormones in Leydig cells.

2.4. Luminescent particles

In vitro studies of cadmium selenium-core quatum dots (CdSeQDs) and polystyrene-based fluorescent particle have been published.

2.4.1. Cadmium selenium-core quantum dots (CdSeQDs)

Quantum dots are colloidal nanocrystalline semiconductors that have unique light-emitting properties and can be used as a novel luminescent material [38]. CdSeQDs are useful as an alternative to fluorescent dyes for use in biological imaging, due to their bright fluorescence, narrow emission, broad UV excitation, and high photostability [39]. An *in vitro* study of CdSeQDs is shown in Table 4.

2.4.1.1. In vitro study of cadmium selenium-core quantum dots (CdSeQDs). The developmental effect of CdSeQDs (approximately 3.5 nm in diameter) was determined using mouse embryos [38]. For water solubilization, the CdSeQDs were surface coupled with mercaptoacetic acid and suspended in PBS. Morulas and blastocysts were obtained from superovulating ICR female mice, which were mated with fertile males of the same strain, by flushing the fallopian tubes on GD 3 and flushing the uterine horns on GD 4, respectively. After incubation of morulas or blastocysts with CdSeQDs for 24 h, an inhibition of the preimplantation development of morulas into blastocysts, increased number of apoptotic cells in the inner cell mass (ICM) of blastocysts ($n = 200$/group) and inhibition of cell proliferation, primarily in the ICM, of blastocysts ($n = 180$/group) at 250 nmol/L and above, and inhibition of the postimplantation development of blastocysts at 125 nmol/L and above were observed. To examine the effect of CdSeQDs on the piostimplantation development of blastocysts, blastocysts ($n = 200$/group) exposed to 0 or 500 nmol/L for 24 h were transferred to recipient ICR mice ($n = 25$/group), which were mated with vasectomized C57BL/6J male mice, on pseudopregnant day (PD) 4 and killed on PD 18. A decreased implantation rate and fetal weight, and increased numbers of embryos with abnormal development and resorptions were observed in the CdSeQDs-treated group. CdSeQDs coated with ZnS had no significant cytotoxic effect on blastocyst development. These findings indicate that CdSeQDs affect adversely pre- and postimplantation embryonic survival and development and the ZnS coating alters the CdSeQD-induced toxicity.

2.4.2. Polystyrene-based fluorescent particles

Fluorescent nanoparticles are promising tools for optical data storage and other technical applications in biochemical, bioanalytical, and medical areas, and were successfully used for immunoassays [40]. An *in vitro* study of fluorescent nanoparticles is shown in Table 4.

2.4.2.1. In vitro study of polystyrene-based fluorescent particles. The effect of ultrafine polystyrene-based fluorescent particles (Molecular Probes Inc.), ranging from 40 nm to over 120 nm in size with different fluorescence colors corresponding to particle size, on mouse embryos was examined [41]. Two-cell stage embryos were incubated with fluorescent nanoparticles at 11.0 million/mL for 4 days, and development was assessed. Untreated embryos incubated for 4 days were further incubated with fluorescent nanoparticles at 11.0 million/mL for 48 h, and the developmental stages of the blastocysts were assessed. No effect of nanoparticles was found on the development of 2-cell stage embryos to the blastocyst stage. There was no effect of nanoparticles on hatching, implantation on the culture dish, or degeneration after additional exposure until the blastocyst stage. Although nanoparticles were internalized, the development of embryos was not affected. Nanoparticles were predominantly found in the trophoblast cells with a few located in the inner cell mass in hatched blastocysts. These findings show that fluorescent nanoparticles did not affect the development of mouse early embryos and suggest that internalized nanoparticles did not affect cellular processes or the expression of factors needed for development.

3. Discussion and conclusions

This paper reviewed the *in vivo* and *in vitro* studies on the reproductive and developmental toxicity of nanomaterials. Although it provides initial information on the potential toxicity of nanomaterials, it should be followed up by relevant hazard studies of nanomaterials.

In vivo studies have showed increased allergic susceptibility in offspring of mouse dams intranasally insufflated with respirable-

size TiO_2, adverse effects on spermatogenesis and histopathological changes in the testes, and changes in gene expression in the brain in mouse offspring after maternal subcutaneous injections of TiO_2 nanoparticles, transfer to rat fetuses of radiolabeled gold nanoparticles and C_{60} after maternal intravenous injection, death and morphological abnormalities in mouse embryos after maternal intraperitoneal injections of C_{60}, and adverse effects on spermatogenesis in mouse offspring after maternal intratracheal instillations of CB nanoparticles. However, these studies were performed with 1–10 administrations of a large bolus and/or a route of exposure not relevant to humans using relatively small numbers of animals. *In vivo* studies should be performed that include doses that closely reflect expected exposure levels. Major routes of exposure to nanoparticles are the respiratory tract, skin, eyes, and gastrointestinal tract. Studies using relevant routes of exposure are needed to clarify the toxicity of nanoparticles. The number of animals per group should be sufficient to allow meaningful interpretation of the data for reproductive and developmental toxicity studies, and a dose–response analysis is also needed to allow more realistic comparisons with actual human exposure. In the studies presented in this review paper, there was a lack of information regarding maternal toxicity. The investigation of maternal toxicity is essential for reproductive and developmental toxicity studies, because the toxicity to offspring may be modified or influenced by toxicity to the mother, and toxicity to offspring often occurs in conjunction with maternal toxicity in animal studies.

Radioactivity was detected in rat fetuses of dams intravenously injected with gold nanoparticles or C_{60}, but unlabeled gold nanoparticles were not detected in mouse fetuses of dams injected intravenously or in the fetal outflow of human placenta. *In vitro* study also revealed some possibility of placental transfer of CoCr particles mediated by a novel mechanism. In terms of developmental toxicity, information on the placental transfer of nanomaterials to offspring of dams given during gestation and lactation is of great interest in interpretation of the data. Measurements of the placental transfer of nanoparticles are an important source of information on the mechanism of action and the risk of nanoparticles, and may help to clarify the reproductive and developmental toxicity of nanoparticles.

As for the effect of nanoparticles on embryonic development, maternally administered C_{60} impaired embryonic development and the results of micromass culture suggest a dysmorphogenic effect of C_{60}. The C_{60} was clearly distributed into the yolk sac. These findings resemble those of developmental toxicity studies of trypan blue, which was teratogenic in mice, rats, hamsters, and guinea pigs [42]. It is generally accepted that teratogenic action of trypan blue in rats is due to its accumulation and interference in the function of the yolk sac, an organ of histotrophic nutrition that provides the principal source of nutrients before the initiation of functional chorio-allantoic placentae. Mice and rats have a yolk sac placenta, which plays a significant role during early in organogenesis. This is not the case for humans and monkeys in which the yolk sac placenta is of insignificant importance. Trypan blue produces malformations in rats and mice due to its accumulation in the yolk sac. This is not possible in humans and monkeys [43].

It is noted that test conducted and reported according to international accepted test guidelines and in compliance with the principles of Good Laboratory Practice (GLP) should have the highest grade of reliability and data for hazard identification must be evaluated considering their quality and adequacy for risk assessment [44]. At present, however, such studies are not available for reproductive and developmental toxicity of nanomaterials. Oberdörster et al. [1] described that studies to assess reproductive effects following pulmonary exposure to nanomaterials should follow protocols similar to OECD guideline 422 for the Testing of Chemicals (Combined Repeated Dose of Toxicity Study with the Reproduction/Developmental Toxicity Screening Test). The OECD guideline 421 for Testing of Chemicals (Reproduction/Developmental Toxicity Screening Test) is also useful to obtain initial information on possible effects on reproduction and development. In these tests, test materials are given to male rats for a minimum of 4 weeks beginning before mating and to females beginning before mating to shortly after parturition of pups. These screening tests are performed using relatively small numbers of animals in the dose groups and do not provide complete information on all aspects of reproduction and development due to the limitation of the exposure period and selectivity of endpoints. The two-generation study, which covers the whole reproductive cycles of at least one generation, may be adequate to evaluate the reproductive and developmental toxicity of nanomaterials. However, the concentrations, populations, and duration of exposure to nanomaterials are different from one another. It is required to modify the exposure period and the endpoints correlated with the exposure period. To further evaluate the reproductive and developmental toxicity of nanomaterials, a more specific test should be designed on a case-by-case basis according to the characterization of human exposure.

In vitro studies revealed high concentrations of TiO_2 nanoparticles to affect the viability and proliferation of mouse Leydig cells, but not the gene expression associated with spermatogenesis. Gold nanoparticles decreased the motility of human sperm, silver, aluminum, and MoO_3 were toxic to mouse spermatogonia stem cells, CoCr nanoparticles damaged DNA of human fibroblast cells, silica nanoparticles inhibited the differentiation of mouse ES cells, C_{60} inhibited the differentiation of mouse midbrain cells, CB decreased the viability of mouse Leydig cells, and CdSeQDs inhibited the pre- and postimplantation development of mouse embryos. In these studies, the concentrations of nanoparticles were very high and unlikely to occur in animal studies. The mechanistic pathways that operate at low realistic concentrations are likely to be different from those operating at very high concentrations when the cell's or organism's defenses are overwhelmed [2]. The findings of these *in vitro* studies are difficult to evaluate because of differences in the chemical composition and sizes of particles, target cells, duration of exposure, endpoints, and exposure concentrations among experiments. *In vivo* studies correlated with results obtained from *in vitro* studies should be performed.

Oxidative stress as a common mechanism for cell damage induced by nanoparticles is well known and a wide range of nanomaterial species have been shown to create reactive oxygen species (ROS) both *in vivo* and *in vitro*. It is suggested that a free radical-induced mechanism or another form of oxidative stress played a role in the developmental toxicity of C_{60} in zebrafish, in which C_{60} caused decreases in the embryonic survival rate, the hatching rate, heartbeat and pericardial edema, and the toxicity was effectively attenuated by adding glutathione, an antioxidant [45]. In mammals, TiO_2 nanoparticles in Leydig cells, Sertili cells, spermatids, and cells of the olfactory bulb and cerebral cortex of pups, and C_{60} in embryos and yolk sac were noted after a maternal administration. In *in vitro* studies, TiO_2 and CB nanoparticles in Leydig cells, Fe_3O_4 and gold nanoparticles in sperm cells, silica nanoparticles in cells of the embryonic body, CoCr nanoparticles in BeWo cells, and fluorescent nanoparticles in trophoblast cells were observed. Determination of the oxidative stress in these cells may help us to understand the reproductive and developmental toxicity of nanoparticles.

The contradicting results obtained from the studies presented in this review may be attributed to the use of different nanomaterials and experimental models, the exposure during different stages of offspring development, and evaluations with different endpoints. It is likely that the size, shapes, chemistry, crystallinity, surface properties, concentration, agglomeration, and dose of nanoparticles are all involved in detecting biological activity. The characterization of